

On the role of the van der Waals interaction in gecko adhesion: A DFT perspective

I.G. Shuttleworth

School of Science and Technology, Nottingham Trent University, Nottingham, NG11 8NS, UK



ARTICLE INFO

Keywords:

van der Waals
Grimme-D2
vdW-DF
Gecko
Glass
PTFE

ABSTRACT

The significance of the van der Waals (vdW) interaction in the adhesion mechanism of geckos to surfaces is estimated quantitatively using dispersion-corrected density functional theory (DFT). A complete survey of the pairwise energies for the elements present in gecko epithelia, soda lime glass and polytetrafluoroethylene (PTFE) shows that the van der Waals interaction plays a minor role in the binding between the atoms in the epithelia and the glass and PTFE substrates. Using a simplified microscopic model for the geckos epithelium, DFT predicts strong (weak) binding between the gecko and glass (PTFE) surfaces, both with and without the vdW interaction. This is in agreement with experimental observations, and is highly suggestive that dispersive interactions only play a minor role in gecko adhesion to glass and PTFE surfaces.

1. Introduction

The gecko needs to be able to grip surfaces in a way that is effective over a wide range of surfaces and in a variety of conditions. The gecko achieves this grip by using large surface-area toes which are covered with micro-/nano-scale fibrils [1,2]. A cogent model of how gecko adhesion occurs at the macroscopic and mesoscopic length scale is starting to emerge and explain some of the more unusual aspects of gecko motivation such as the apparent ability of geckos to move more rapidly on wet surfaces than on the same dry surface.

However, some controversy exists over the exact nature of the microscopic interactions between these fibrils and the surface supporting the gecko. Recent experimental studies [3] have suggested that contact electrification is the more important microscopic mechanism, contradicting earlier studies [4] which applied mesoscopic length-scale models [5] to experimental results and inferred that the van der Waals (vdW) or dispersion interaction is the more important.

The vdW interaction is a true quantum phenomenon, causing a net attraction between fragments of electrons in many-electron systems. Computationally, vdW forces have become significant since the early 1990's [6] after the successful deployment of the Local Density and Generalised Gradient Approximations (LDA and GGA, respectively) in Density Functional Theory (DFT). As a result, their ubiquity and importance in a range of applied phenomena scaling across the biological sciences, chemistry, engineering and physics are only now being quantified.

The relationship between the van der Waals interaction and the

phenomenon of contact electrification is subtle. In DFT terms, then vdW interaction can be treated separately to permanent transfers of charge. This means that the formation of, for example, surface double layers and the associated terms which develop during contact electrification can be predicted by DFT with and without the inclusion of vdW terms. Consequently, a quantitative comparison between charge transfer and vdW effects can be made directly using DFT and it is this approach which will be used in the current work.

In first part of the current work, the pair-wise interaction energy will be estimated using both dispersion corrected and non-dispersion corrected DFT across a range of elements present in gecko epithelia, and in glass and polytetrafluoroethylene (PTFE). In the second part of this work the binding energy of the component molecules of gecko epithelia with glass and PTFE will be estimated both with and without dispersion, and the subsequent discussion will focus on the relative importance of the dispersion correction to these pair-wise and binding energies compared to the energy of the non-dispersion corrected self-consistent field.

1.1. Computational methods

The DFT simulations presented in this work were performed using the Quantum Espresso package [9]. For all simulations, a wave-function kinetic energy cut-off of 75 Ry and a charge density/potential cut-off of 900 Ry were used. A first-order Methfessel-Paxton smearing of 0.02 Ry [10] was also used throughout this work. For all elements, the PAW pseudo-potentials [11] were generated using the

E-mail address: ian.shuttleworth@ntu.ac.uk.

<https://doi.org/10.1016/j.rinma.2020.100080>

Received in revised form 16 January 2020; Accepted 29 February 2020

Available online xxxx

2590-048X/© 2020 The Author(s). Published by Elsevier B.V. This is an open access article under the CC BY-NC-ND license (<http://creativecommons.org/licenses/by-nc-nd/4.0/>).

Perdew-Burke-Ernzerhof (PBE) exchange-correlation functional.

The vdW interaction was estimated using two methods: the Grimme-D2 approach [12,13] and the non-local vdW-DF method [14]. Though the more empirical of the two approaches, the Grimme-D2 method is particularly relevant in the current investigations because it has been shown to perform well for systems which contain covalent bonds [15] as well as for systems which are dominated by dispersion forces. Comparatively, the vdW-DF method is both non-empirical and non-local and is consequently significantly more computationally costly. However, the vdW-DF method is significantly more rigorous than the Grimme-D2 approach so will be used as a benchmark in the current investigations.

Following the Grimme-D2 approach the energy of the system can be written in the separable form

$$E_{\text{DFT-D}} = E_{\text{DFT}} + E_{\text{disp}} \quad (1)$$

E_{DFT} is the non-dispersion corrected Kohn-Sham energy and E_{disp} is the dispersion correction given by [12].

$$E_{\text{disp}} = -s_6 \sum_{i=1}^{N_{\text{at}}-1} \sum_{j=i+1}^{N_{\text{at}}} \frac{C_6^{ij}}{r^6} f_{\text{dmp}}(r) \quad (2)$$

s_6 is a scaling factor which depends on the choice of density-functional used, C_6^{ij} is the dispersion coefficient for the atom pair ij , $f_{\text{dmp}}(r)$ is a damping function which depends on the inter-atomic distance r and N_{at} is the total number of atoms in the system. The C_6^{ij} are calculated by the geometric mean of the atomic terms

$$C_6^{ij} = \sqrt{C_6^i C_6^j} \quad (3)$$

The atomic terms from Refs. [12] are summarised in Table 1 for the elements considered in the current work.

In order to calculate the pairwise-interaction energies between atoms, pairs of atoms were placed in a $40 \times 40 \times 40 \text{ \AA}^3$ cell and the non-dispersion and dispersion corrected Kohn-Sham energies - E_{pair} and $E_{\text{pair,vdW}}$, respectively - were calculated as a function of the distance between the atoms r . During these simulations, Γ k-point sampling was used.

Eqns. (1) and (2) show that the contribution of dispersion to the total binding energy of a multi-atom system can be estimated by adding the pair-wise contributions defined in Eqn. (2). This is because Eqns. (1) and (2) show explicitly that the pairwise dispersion interaction doesn't saturate with atom numbers, and that the binding energy between a molecule and an extended surface or a polycrystalline sample can be thought of as the sum of the energies due to the non-dispersion corrected self-consistent field, and a dispersion correction.

The importance of the dispersion correction - i.e. the importance of E_{DFT} compared to $E_{\text{DFT-D}}$ - when geckos walk across glass and polytetrafluoroethylene (PTFE) surfaces was estimated using a combination of dispersion corrected and non-dispersion corrected simulations. Glass and PTFE were chosen as substrates because experimentally geckos are seen to adhere to glass [7] but not to PTFE [8]. The most commonly occurring form of glass is soda lime glass, which is approximately 75% silicon dioxide (SiO_2). The remaining 25% of the glass is composed of sodium oxide (Na_2O) and calcium oxide (CaO). This material most commonly occurs in polycrystalline form. To approximate interaction between molecules and a polycrystalline glass sample, the interactions between molecules and the (111), (110) and (100) surfaces of the SiO_2 , Na_2O and CaO crystals was calculated. These surfaces were chosen

because they are amongst the lowest energy, and therefore surface micro-facets of the polycrystalline sample are most likely to be formed of them.

Silicon dioxide (SiO_2) is shown in Fig. 1 (a). The experimental quartz structure of this material was taken from the American Mineralogist Crystal Structure Database [16]. Similarly, the sodium oxide (Na_2O) (antifluorite) and calcium oxide (CaO) (rocksalt) nanoparticles are shown in Fig. 1(b-c). For each bulk sample the lattice parameter was relaxed to minimise the Kohn-Sham, or dispersion corrected Kohn-Sham, energy. Each surface was then fully relaxed before simulating the adsorption molecules. For all simulations of these oxides the +U correction was included.

To simulate the interaction between the geckos epithelium and PTFE, a slab of PTFE was formed from individual PTFE strands. Fig. 1 (d) shows a single strand of PTFE $(\text{CF}_2)_n$. In this case a small number of strands (up to 4) we lain next to another and allowed to relax locally but not to react, before estimating interaction strengths.

Substrate slabs of 5-7 layer thickness with orthogonal surface unit cells of approximately $20 \times 20 \text{ \AA}^2$ were used to minimise the interaction between adjacent adsorbed molecules. Adjacent slabs were separated by a distance of 40 \AA . Symmetric adsorption was simulated with molecules pattering either side of each slab.

Fig. 2 shows the difference δE in the total energy of an oxygen-terminated $\text{SiO}_2(111)$ slab calculated using k-point sampling of $n_k \times n_k \times 1$ and the total energy of the same slab using k-point sampling of $10 \times 10 \times 1$. These simulations were performed to ensure that an adequate k-sampling rate was used in these investigations. Convergence was seen by $n_k = 4$ for the all substrates, and earlier - $n_k = 2$ - for the PTFE slab. Consequently $(6 \times 6 \times 1)$ k-point sampling was used throughout these investigations.

The epithelial layers of gecko are formed of β -keratin sheets [17]. The component molecules of these sheets are glycine ($\text{NH}_2\text{CH}_2\text{COOH}$) and cysteine ($\text{HO}_2\text{CCH}(\text{NH}_2)\text{CH}_2\text{SH}$) molecules. These molecules are shown

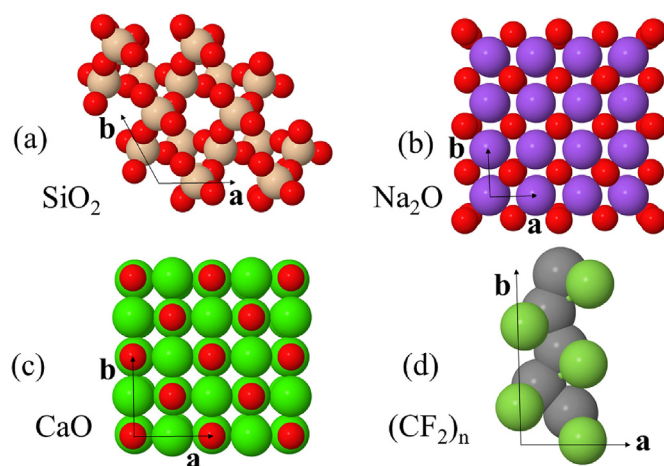


Fig. 1. The ideally bulk terminated (a) $\text{SiO}_2(0001)$, (b) $\text{Na}_2\text{O}(001)$, and (c) $\text{CaO}(001)$ surfaces used in the current work to simulated the interaction between the gecko and soda lime glass. The non-orthogonal primitive unit cell is used for (a) but orthogonal unit cells are used for (b-c). (d) shows a single strand of PTFE $(\text{CF}_2)_n$ used in the simulations between geckos and the polymer. In (a-c) the oxygen atoms are denoted by red spheres, and the Si, Na and Ca atoms are denoted by dull orange, purple and green atoms, respectively. In (d) the C and F atoms are denoted by dull and light green atoms, respectively.

Table 1

Summary of Grimme C_6 parameters (in $\text{Jnm}^6\text{mol}^{-1}$) [12].

| Element | C | O | H | N | S | Si | Na | Ca | F |
|---------|------|------|------|------|------|------|------|-------|------|
| C_6 | 1.75 | 0.70 | 0.14 | 1.23 | 5.57 | 9.23 | 5.71 | 10.80 | 0.75 |

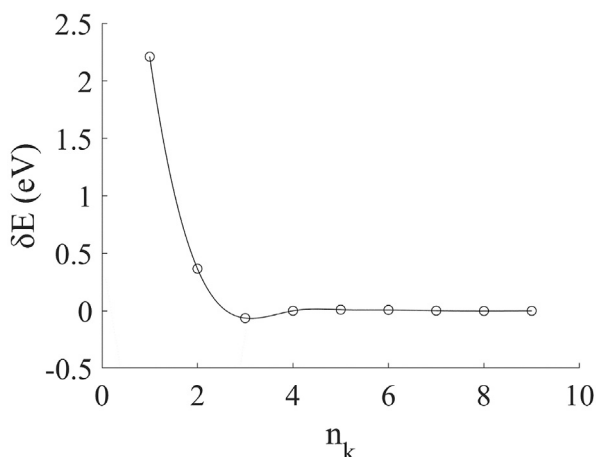


Fig. 2. Difference δE in the total energy of an oxygen-terminated $\text{SiO}_2(111)$ slab calculated using k -point sampling of $n_k \times n_k \times 1$ and the total energy of the same slab using k -point sampling of $10 \times 10 \times 1$. Similar curves were obtained for the $\text{SiO}_2(110)$ and the $\text{SiO}_2(100)$ slabs, and for slabs of the other substrates.

in Fig. 3 and the interaction between these molecules and the various substrates was calculated to estimate the interaction between the β -keratin sheet and these substrates. To most accurately mimic the action of the β -keratin sheet against the substrate during gecko walking, only the interaction between glycine and cysteine molecules with their molecular axes parallel to the substrate are considered i.e. the C–C–N (C–C–C) chains of the glycine (cysteine) molecules were oriented parallel to the surface plane.

The surface binding energies of the glycine and cysteine molecules were calculated in the absence of the van der Waals correction using

$$E_{\text{bind}} = E_{\text{ads/subs}} - \frac{1}{2}(2E_{\text{ads}} + E_{\text{subs}}) \quad (4)$$

$E_{\text{ads/subs}}$ is the Kohn-Sham energy of the glycine or cysteine bearing slab, and E_{ads} and E_{subs} are the energies of the gas-phase molecule and clean surface, respectively. The factors of 2 and $\frac{1}{2}$ account for the presence of adsorbate molecules on either side of the slab. The dispersion-corrected surface binding energy $E_{\text{bind;vdW}}$ was defined identically to Eqn. (4), though using dispersion-corrected energies.

To mimic the range of registries between the glycine and cysteine molecules and the various substrates, the mean binding energy E_{bind} was calculated by constraining the centre mass of the glycine or the cysteine molecule to $(c_1\mathbf{a}, c_2\mathbf{b})$ where \mathbf{a} and \mathbf{b} are defined in Fig. 1, and c_1 and c_2 each took values of $(0, 1/3, 2/3)$. In this way a lattice of nine different positions were defined across each surface. At each position, the glycine and cysteine molecules were allowed to relax into the local minimum.

The difference in the binding energies between the dispersion corrected and non-dispersion corrected binding energies was

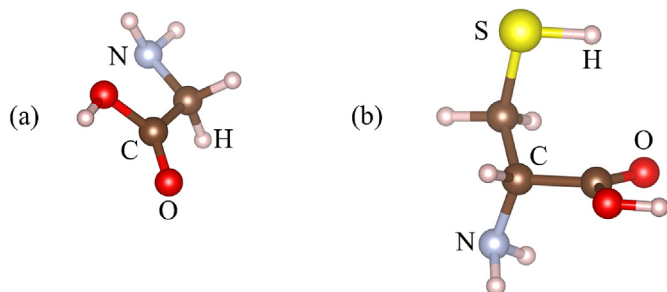


Fig. 3. The (a) glycine, and (b) cysteine molecules used to approximate the β -keratin sheets of the geckos epithelial layer.

$$\delta_{\text{bind}} = 2 \left| \frac{E_{\text{bind}} - E_{\text{bind;vdW}}}{E_{\text{bind}} + E_{\text{bind;vdW}}} \right| \times 100\% \quad (5)$$

The $E_{\text{bind;vdW}}$ denote binding energies estimated using dispersion corrected simulations, either by the Grimme-D2 or by the vdW-DF approach.

2. Results and discussion

The upper panels in Fig. 4(a–e) show the pairwise non-dispersion corrected Kohn-Sham energies E_{pair} between atoms in the glycine and cysteine molecules - C, H, N, O and S - and the Si, O, Na, Ca, C and F atoms of the substrates as a function of the inter-atomic separation r . $E_{\text{pair}}(r)$ has a minimum at the equilibrium pair separation $r_{\text{pair}}^{\text{eqblrm}}$. The magnitude of these minima $E_{\text{pair}}^{\text{min}}$ are presented in Table 2.

The lower panels in Fig. 4(a–e) show the difference between $E_{\text{pair}}(r)$ and the dispersion corrected pairwise Kohn-Sham energies $E_{\text{pair;DFT-D}}$. For these curves the dispersion correction was performed using the Grimme-D2 method. The curves in these panels show a maximum at inter-atomic separations greater than the equilibrium pair separation $r_{\text{pair}}^{\text{eqblrm}}$.

The magnitudes of maximum difference in energies are presented in Table 3 for simulations that used the Grimme-D2 approach, and also for simulations that used the vdW-DF approach. These energy differences show that the pair-wise energy difference between the dispersion and non-dispersion energy simulations are sensitive to the inter-atomic separation r , and that the magnitude of this energy difference is much less than the total interaction energy at equilibrium separation for all of the presented pairs of atoms. This indicates that for these particular combinations of atom pairs, the vdW correction does not contribute significantly to their total interaction energy, suggesting that the vdW interaction is only expected to play a minor role in the binding between the gecko (i.e. the glycine and cysteine components of the simulations) and the glass and PTFE substrates. The strong level of consistency between the Grimme-D2 and the vdW-DF simulations also show that, for this particular set of molecules and surfaces the Grimme parameterisation is reasonable and that the errors in this approach are negligible when compared to the total pairwise binding energies between pairs of atoms.

Table 4 summarises the mean surface binding energies E_{bind} of glycine and cysteine to the low index SiO_2 , Na_2O , CaO facets and to PTFE sheets using both non-van der Waals corrected DFT and both the Grimme-D2 and vdW-DF corrections. This summary is consistent with the pairwise energies presented in Table 3 as Table 4 shows that the difference in binding energies between the dispersion and non-dispersion binding energies δ_{bind} is minor compared to contribution to the binding energy calculated using the non-dispersion corrected self-consistent field. The observations in Tables 3 and 4 can be rationalised by considering the Grimme-D2 model presented in Eqns. (1)–(3) and the C_6 coefficients. According to the Grimme-D2 model the magnitude of the dispersion correction depends on C_6 as well as the inter-atomic separation. The C_6 dependence is most clearly shown in Eqn. (3) where larger values of the parameter for both atoms are required to make the total interaction significant. These larger values of C_6 are only evident for Si, Na and Ca (Table 1) so though this interaction may be present in the substrate before adsorption it isn't present in interactions between either glycine or cysteine and the substrate and therefore doesn't cause a significant energy shift during their adsorption.

These results support a model of gecko adhesion to glass and PTFE that is not strongly dependent on the vdW interaction. The more significant interaction in these systems, shown quantitatively in both the pairwise studies and the molecule-surface studies, develops from the self-consistent field and this field's prediction of permanent charge transfer. The DFT treatment also shows that the interaction between glycine and cysteine and the glass facets (SiO_2 , Na_2O and CaO) are stronger than their interaction with PTFE. This is evidence by comparing the values of the

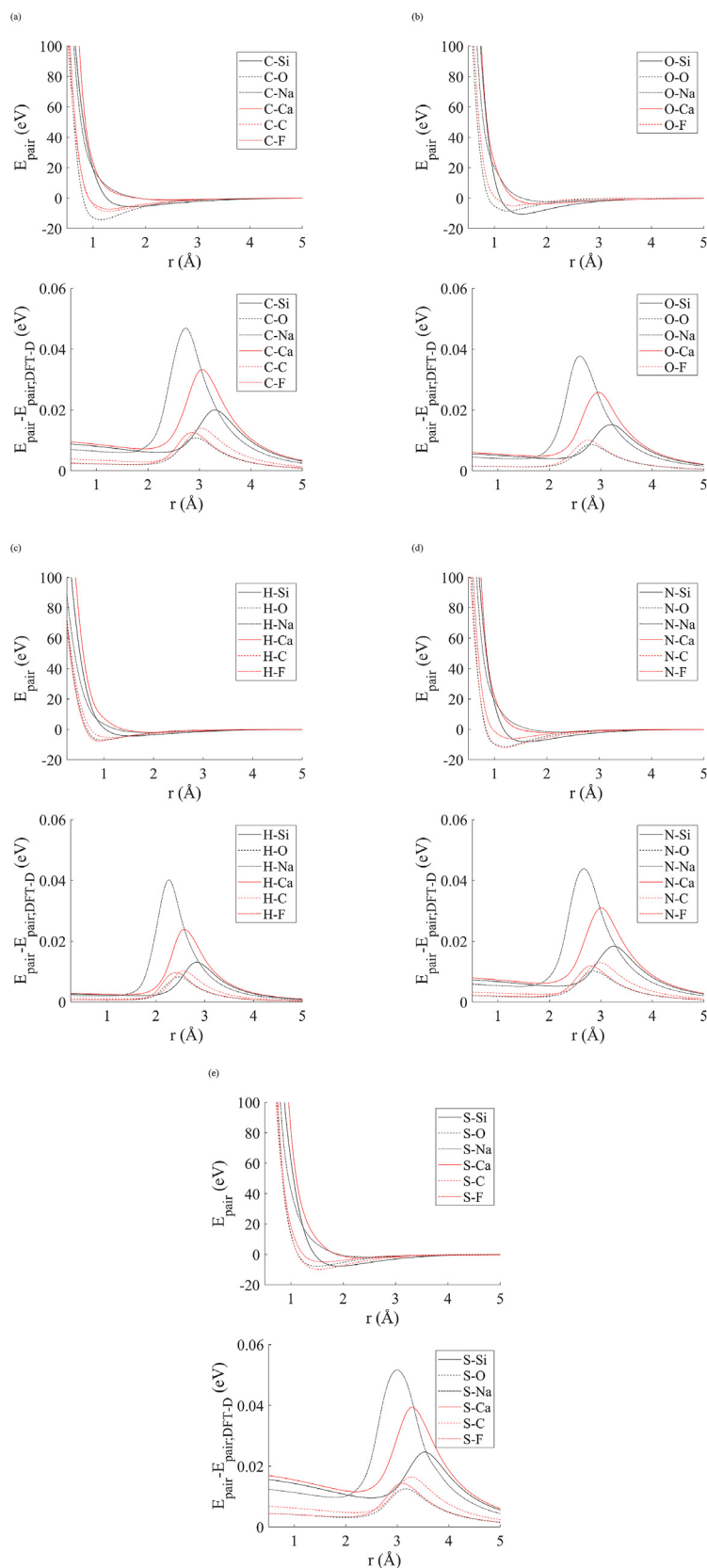


Fig. 4. Pair-wise interaction energies E_{pair} , and the difference energies $E_{\text{pair}} - E_{\text{pair,DFT-D}}$ between (a) C, (b) O, (c) H, (d) N, and (e) S, and the elements shown in the legends. E_{pair} ($E_{\text{pair,DFT-D}}$) was determined without (with) the inclusion of the dispersion interaction. The dispersion interaction was estimated using the Grimme-D2 [12,13] method.

Table 2

Summary of minimum pairwise interaction energies $E_{\text{pair}}^{\text{min}}$ and equilibrium pair separation distances $r_{\text{pair}}^{\text{eqbrm}}$ between (a) C, (b) O, (c) H, (d) N, and (e) S, and the other elements listed in the second and subsequent rows of each table. Energies are in eV and distances in Å.

| C | $E_{\text{pair}}^{\text{min}}$ | $r_{\text{pair}}^{\text{eqbrm}}$ |
|-----|--------------------------------|----------------------------------|
| (a) | | |
| Si | -5.6990 | 1.7507 |
| O | -14.1620 | 1.1584 |
| Na | -1.2693 | 2.5068 |
| Ca | -1.1834 | 2.4311 |
| C | -8.6381 | 1.2831 |
| F | -7.2869 | 1.3096 |
| O | $E_{\text{pair}}^{\text{min}}$ | $r_{\text{pair}}^{\text{eqbrm}}$ |
| (b) | | |
| Si | -10.5540 | 1.5257 |
| O | -8.5147 | 1.2682 |
| Na | -2.3746 | 2.0738 |
| Ca | -3.8709 | 1.8380 |
| F | -5.0462 | 1.3582 |
| H | $E_{\text{pair}}^{\text{min}}$ | $r_{\text{pair}}^{\text{eqbrm}}$ |
| (c) | | |
| Si | -4.2869 | 1.5450 |
| O | -6.8303 | 0.9307 |
| Na | -2.0692 | 1.8994 |
| Ca | -1.9604 | 1.9953 |
| C | -5.2625 | 1.1597 |
| F | -7.6176 | 0.8980 |
| N | $E_{\text{pair}}^{\text{min}}$ | $r_{\text{pair}}^{\text{eqbrm}}$ |
| (d) | | |
| Si | -8.1051 | 1.6062 |
| O | -11.3795 | 1.2138 |
| Na | -1.7112 | 2.2682 |
| Ca | -2.2844 | 2.0828 |
| C | -11.9926 | 1.1913 |
| F | -6.1701 | 1.3353 |
| S | $E_{\text{pair}}^{\text{min}}$ | $r_{\text{pair}}^{\text{eqbrm}}$ |
| (e) | | |
| Si | -7.7610 | 1.9217 |
| O | -7.8108 | 1.4977 |
| Na | -1.7597 | 2.4977 |
| Ca | -2.1091 | 2.4221 |
| C | -9.7977 | 1.5414 |
| F | -4.9620 | 1.6323 |

mean surface binding energies E_{bind} in Table 4 for the PTFE systems with those for the oxide surfaces. The consistently higher binding energies for the oxides is consistent with the experimental observation that geckos adhere to glass but not to PTFE, and is further evidence that the permanent charge transfer model is a more consistent approach to gecko adhesion to surfaces.

3. Conclusions

The interaction between gecko epithelia and both soda lime glass and polytetrafluoroethylene (PTFE) have been investigated both with and without corrections for the van der Waals (vdW) interaction using density functional theory (DFT). In this work, which has focussed on the energetics of the interaction, studies of the pair-wise interactions between atoms in the glycine and cysteine of the gecko epithelium, and those which can found across the surfaces of polycrystalline soda lime glass and PTFE have shown that the vdW interaction contributes only nominally, up to at most approximately 0.1%, of the total binding energy between the atoms. It was also shown that this correction is extremely sensitive to the distance between the atoms. Small changes (of the order of ± 0.5 Å) in the atom-atom separation were shown to reduce the

Table 3

Summary of the maximum differences between the minimum pairwise interaction energies $E_{\text{pair}}^{\text{min}}$, $E_{\text{pair,DFT-D}}^{\text{min}}$ and $E_{\text{pair,vdW-DF}}^{\text{min}}$ and the equilibrium pair separations $r_{\text{pair}}^{\text{eqbrm}}$, $r_{\text{pair,DFT-D}}^{\text{eqbrm}}$ and $r_{\text{pair,vdW-DF}}^{\text{eqbrm}}$ between (a) C, (b) O, (c) H, (d) N, and (e) S, and the other elements listed in the second and subsequent rows of each table. The subscripts 'DFT-D' and 'vdW-DF' denote quantities estimated using the Grimme-D2 [12,13], and vdW-DF [14] treatments of the van der Waals interaction, respectively. A hyphen '-' indicates a difference in lengths of < 0.0001 Å. All energies are in eV and distances in Å.

| C | $E_{\text{pair}}^{\text{min}}$ | $E_{\text{pair,DFT-D}}^{\text{min}}$ | $E_{\text{pair,vdW-DF}}^{\text{min}}$ | $r_{\text{pair}}^{\text{eqbrm}}$ | $r_{\text{pair,DFT-D}}^{\text{eqbrm}}$ | $r_{\text{pair,vdW-DF}}^{\text{eqbrm}}$ |
|-----|--------------------------------|--------------------------------------|---------------------------------------|----------------------------------|--|---|
| (a) | | | | | | |
| Si | 0.0065 | | 0.0032 | - | | 0.0020 |
| O | 0.0022 | | -0.0851 | - | | -0.0137 |
| Na | 0.0381 | | 0.0000 | -0.0307 | | - |
| Ca | 0.0110 | | -0.0006 | -0.0069 | | 0.0010 |
| C | 0.0032 | | 0.0500 | - | | 0.0010 |
| F | 0.0022 | | -0.0339 | - | | -0.0037 |
| O | $E_{\text{pair}}^{\text{min}}$ | $E_{\text{pair,DFT-D}}^{\text{min}}$ | $E_{\text{pair,vdW-DF}}^{\text{min}}$ | $r_{\text{pair}}^{\text{eqbrm}}$ | $r_{\text{pair,DFT-D}}^{\text{eqbrm}}$ | $r_{\text{pair,vdW-DF}}^{\text{eqbrm}}$ |
| (b) | | | | | | |
| Si | 0.0044 | | -0.0025 | - | | - |
| O | 0.0014 | | 0.0538 | - | | -0.0119 |
| Na | 0.0099 | | -0.0031 | -0.0039 | | 0.0010 |
| Ca | 0.0047 | | -0.0020 | - | | 0.0029 |
| F | 0.0014 | | 0.0620 | - | | 0.0267 |
| H | $E_{\text{pair}}^{\text{min}}$ | $E_{\text{pair,DFT-D}}^{\text{min}}$ | $E_{\text{pair,vdW-DF}}^{\text{min}}$ | $r_{\text{pair}}^{\text{eqbrm}}$ | $r_{\text{pair,DFT-D}}^{\text{eqbrm}}$ | $r_{\text{pair,vdW-DF}}^{\text{eqbrm}}$ |
| (c) | | | | | | |
| Si | 0.0021 | | -0.0007 | - | | -0.0009 |
| O | 0.0006 | | 0.0805 | - | | 0.0343 |
| Na | 0.0160 | | -0.0006 | -0.0187 | | -0.0010 |
| Ca | 0.0050 | | 0.0000 | -0.0039 | | -0.0009 |
| C | 0.0010 | | -0.0184 | - | | -0.0147 |
| F | 0.0006 | | 0.1875 | - | | 0.0205 |
| N | $E_{\text{pair}}^{\text{min}}$ | $E_{\text{pair,DFT-D}}^{\text{min}}$ | $E_{\text{pair,vdW-DF}}^{\text{min}}$ | $r_{\text{pair}}^{\text{eqbrm}}$ | $r_{\text{pair,DFT-D}}^{\text{eqbrm}}$ | $r_{\text{pair,vdW-DF}}^{\text{eqbrm}}$ |
| (d) | | | | | | |
| Si | 0.0057 | | -0.0002 | - | | 0.0088 |
| O | 0.0018 | | -0.0500 | - | | -0.0216 |
| Na | 0.0195 | | 0.0004 | -0.0173 | | -0.0010 |
| Ca | 0.0065 | | 0.0052 | -0.0010 | | - |
| C | 0.0028 | | -0.0368 | - | | -0.0186 |
| F | 0.0018 | | -0.0350 | - | | -0.0125 |
| S | $E_{\text{pair}}^{\text{min}}$ | $E_{\text{pair,DFT-D}}^{\text{min}}$ | $E_{\text{pair,vdW-DF}}^{\text{min}}$ | $r_{\text{pair}}^{\text{eqbrm}}$ | $r_{\text{pair,DFT-D}}^{\text{eqbrm}}$ | $r_{\text{pair,vdW-DF}}^{\text{eqbrm}}$ |
| (e) | | | | | | |
| Si | 0.0109 | | -0.0022 | - | | - |
| O | 0.0036 | | -0.0250 | - | | -0.0044 |
| Na | 0.0226 | | 0.0021 | -0.0157 | | -0.0010 |
| Ca | 0.0122 | | 0.0004 | -0.0010 | | -0.0030 |
| C | 0.0054 | | -0.0038 | - | | -0.0010 |
| F | 0.0035 | | 0.0063 | - | | -0.0053 |

significance of the vdW to practically zero. The empirical Grimme-D2 approach has been shown to be a reasonable parameterisation for the systems modelled in the current investigation by comparison with the non-empirical, non-local vdW-DF approach.

Simulations of the adsorption of both glycine and cysteine on the low index faces of SiO_2 , Na_2O and CaO – the crystalline components of soda lime glass – and on PTFE sheets were consistent with these pairwise studies as they demonstrated that the fractional difference between the binding energies obtained with and without the van der Waals correction was again nominal. The relative lack of importance of the van der Waals interaction in these adsorption systems was reconciled quantitatively through a discussion of the values of the C6 parameters used in the Grimme-D2 approach [12,13] which shows quantitatively that the dispersion interaction between the C, H, N, O and S of the glycine and cysteine adsorbates, and the Si, O, Na, Ca, C and F of the substrates is minor.

Table 4

Summary of the mean surface binding energies E_{bind} (in eV) during glycine and cysteine adsorption to the (111), (110) and (100) surfaces of SiO_2 , Na_2O , CaO , and to PTFE $(\text{CF}_2)_n$, determined using both non-van der Waals corrected DFT and both the Grimme-D2 and vdW-DF corrections. The two percentages in brackets after shows δ_{bind} the fractional difference between binding energies calculated with and without the van der Waals correction. These differences – to the left and right of the hyphen - were obtained using the Grimme-D2 [12,13] and vdW-DF [14] treatments of the van der Waals interaction, respectively.

| Substrate | | Adsorbate | |
|---------------------------------|-------|---------------------|---------------------|
| | | Glycine | Cysteine |
| SiO_2 (Non-terminated) | (111) | −7.03 (0.37–0.37%) | −9.35 (0.43–0.42%) |
| | (100) | −20.04 (0.37–0.39%) | −13.82 (0.45–0.46%) |
| | (110) | −14.30 (0.34–0.35%) | −8.17 (0.41–0.42%) |
| SiO_2 (Terminated) | (111) | −8.61 (0.21–0.21%) | −10.94 (0.31–0.32%) |
| | (100) | −19.05 (0.22–0.23%) | −11.96 (0.28–0.27%) |
| | (110) | −13.64 (0.22–0.22%) | −5.23 (0.32–0.33%) |
| Na_2O | (111) | −16.47 (0.20–0.21%) | −23.84 (0.22–0.23%) |
| | (100) | −11.82 (0.18–0.19%) | −25.05 (0.21–0.22%) |
| | (110) | −5.31 (0.21–0.20%) | −17.57 (0.21–0.22%) |
| CaO | (111) | −28.44 (0.31–0.32%) | −27.16 (0.33–0.34%) |
| | (100) | −17.77 (0.33–0.33%) | −21.95 (0.34–0.35%) |
| | (110) | −12.52 (0.33–0.32%) | −16.58 (0.34–0.36%) |
| PTFE | – | −1.85 (0.17–0.17%) | −1.12 (0.16–0.17%) |

References

- [1] A.P. Russell, A.Y. Stark, T.E. Higham, The integrative biology of gecko adhesion: historical review, current understanding, and grand challenges, *Integr. Comp. Biol.* 59 (1) (2019) 101–116.
- [2] P.H. Niewiarowski, A.Y. Stark, A. Dhinojwala, Sticking to the story: outstanding challenges in gecko-inspired adhesives, *J. Exp. Biol.* 219 (2016) 912–919.
- [3] H. Izadi, K.M.E. Stewart, A. Penlidis, Role of contact electrification and electrostatic interactions in gecko adhesion, *J. R. Soc. Interface* 11 (2014) 20140371.
- [4] K. Autumn, M. Sitti, Y.A. Liang, A.M. Peattie, W.R. Hansen, S. Sponberg, T.W. Kenny, R. Fearing, J.N. Israelachvili, R.J. Full, Evidence for van der Waals adhesion in gecko setae, *Proc. Natl. Acad. Sci. Unit. States Am.* 99 (19) (2002) 12252–12256.
- [5] J.N. Israelachvili, *Intermolecular and Surface Forces*, Elsevier, 2011.
- [6] J. Hermann, R.A. DiStasio Jr., A. Tkatchenko, First-principles models for van der Waals interactions in molecules and materials: concepts, theory, and applications, *Chem. Rev.* 117 (2017) 4714–4758.
- [7] K. Autumn, N. Gravish, Gecko adhesion: evolutionary nanotechnology, *Phil. Trans. R. Soc. A* 366 (2008) 1575–1590.
- [8] A.Y. Stark, D.M. Dryden, J. Olderman, K.A. Peterson, P.H. Niewiarowski, R.H. French, A. Dhinojwala, Adhesive interactions of geckos with wet and dry fluoropolymer substrates, *J. R. Soc. Interface* 12 (2015) 20150464.
- [9] P. Giannozzi, O. Andreussi, T. Brumme, O. Bunau, M. Buongiorno Nardelli, M. Calandra, R. Car, C. Cavazzoni, D. Ceresoli, M. Cococcioni, N. Colonna, I. Carnimeo, A. Dal Corso, S. de Gironcoli, P. Delugas, R.A. DiStasio Jr., A. Ferretti, A. Floris, G. Fratesi, G. Fugallo, R. Gebauer, U. Gerstmann, F. Giustino, T. Gorni, J. Jia, M. Kawamura, H.-Y. Ko, A. Kokalj, E. Küçükbenli, M. Lazzeri, M. Marsili, N. Marzari, F. Mauri, N.L. Nguyen, H.-V. Nguyen, A. Otero-de-la-Roza, L. Paulatto, S. Poncè, D. Rocca, R. Sabatini, B. Santra, M. Schlipf, A.P. Seitsonen, A. Smogunov, I. Timrov, T. Thonhauser, P. Umari, N. Vast, X. Wu, S. Baroni, Advanced capabilities for materials modelling with Quantum ESPRESSO, *J. Phys. Condens. Matter* 29 (2017) 465901.
- [10] M. Methfessel, A.T. Paxton, High-precision sampling for Brillouin-zone integration in metals, *Phys. Rev. B Condens. Matter* 40 (1989) 3616–3621.
- [11] A. Dal Corso, Pseudopotentials periodic table: from H to Pu, *Comput. Mater. Sci.* 95 (2014) 337–350.
- [12] S. Grimme, Semiempirical GGA-type density functional constructed with a long-range dispersion correction, *J. Comput. Chem.* 27 (2006) 1787–1799.
- [13] V. Barone, M. Casarin, D. Forrer, M. Pavone, M. Sambi, A. Vittadini, Role and effective treatment of dispersive forces in materials: polyethylene and graphite crystals as test cases, *J. Comput. Chem.* 30 (2009) 934–939.
- [14] M. Dion, H. Rydberg, E. Schröder, D.C. Langreth, B.I. Lundqvist, Van der Waals density functional for general geometries, *Phys. Rev. Lett.* 92 (2004) 246401.
- [15] S. Grimme, J. Antony, S. Ehrlich, H. Krieg, A consistent and accurate ab initio parametrization of density functional dispersion correction (DFT-D) for the 94 elements H-Pu, *J. Chem. Phys.* 132 (15) (2010) 154104.
- [16] R.T. Downs, M. Hall-Wallace, *Am. Mineral.* 88 (2003) 247–250.
- [17] L. Alibardi, Review: mapping proteins localized in adhesive setae of the tokay gecko and their possible influence on the mechanism of adhesion, *Protoplasma* 255 (2018) 1785–1797.